Numerical investigation of thermal discharge to coastal areas: A case study in South Italy

Published Version:
Gaeta, M.G., Samaras, A.G., Archetti, R. (2020). Numerical investigation of thermal discharge to coastal areas: A case study in South Italy. ENVIRONMENTAL MODELLING & SOFTWARE, 124, 1-13 [10.1016/j.envsoft.2019.104596].

Availability:
This version is available at: https://hdl.handle.net/11585/784349 since: 2020-12-14

Published:
DOI: http://doi.org/10.1016/j.envsoft.2019.104596

Numerical investigation of thermal discharge to coastal areas: a case study in South Italy

Maria Gabriella Gaeta [a,*], Achilleas G. Samaras [b], Renata Archetti[a]

[a] *Department of Civil, Chemical, Environmental and Materials Engineering, University of Bologna, Bologna - Italy*

[b] *Department of Civil Engineering, Aristotle University of Thessaloniki, Thessaloniki – Greece*

* Corresponding author. Tel: +39 051 2090508

E-mail address: g.gaeta@unibo.it (M.G. Gaeta)

HIGHLIGHTS

- Thermal release dynamics in sea was studied by a wave – 3D-hydrodynamics model
- Sea temperature measurements were used to calibrate the model
- Sensitivity analyses highlighted the importance of including wave – wind modelling
- Turbulence, vertical diffusion and wind drag coefficients were found key-parameters
- Environmental and operational scenarios revealed changes in thermal plume

ABSTRACT

Coupled wave – 3D-hydrodynamics model runs are performed to investigate thermal discharge release to coastal areas by means of including nearshore effects of wave-current dynamics. The study area comprises the vicinity of a power plant at Cerano, in South Italy, where cooling industrial waters are released to the sea. The implemented model is calibrated by using temperature measurements and sensitivity analyses are carried out for various relevant drivers and input parameters. Afterwards, the effect of thermal discharge is investigated through distinct hypothetical scenarios for a combination of metocean conditions and operational features of the power plant (modifying water discharge and temperature at its outlet). The model results of this representative array of conditions are intercompared and evaluated on the basis of heat dispersion rate and areas of influence, providing with useful insights on the numerical simulation of the process and the potential effects for the specific coastal area.

Keywords: thermal pollution; 3D numerical model; sea temperature; wave action; mixing area.

1. Introduction

Sea surface temperature (SST) is considered as one of the most important parameters in observing ecosystem conditions for marine/coastal environments (Azmi et al., 2015; Brando et al., 2015), with the sustainability of their habitats being largely dependent on water quality.

Thermal pollution is defined as any deviation of the environment temperature due to industrial cooling cycles or natural discharges of cold fluid into water bodies (Dodds and Whiles, 2010). Although thermal pollution may refer to the decrease of water temperature as well, the term is usually associated with the effects of the increase in water temperature in rivers, lakes and coastal areas, as well as the consequent decrease of the concentration of dissolved oxygen (DO) degrading water quality.

Generally, the mean water body temperature may not be significantly affected by the introduction of thermal discharges due to its large heat capacity, but eventually steep rises in local temperature disturb the aquatic flora and fauna in it, modifying the ecological balance in the affected areas. Indeed, abrupt changes in water temperature, known as “thermal shocks”, deeply damage the marine ecosystem, leading to significant decrease of DO concentration in water up to biodiversity alteration, such as increased bacteria levels, changes in metabolism, reproduction, denaturing of life-supporting enzymes and increase of mortality for aquatic species (Lardicci et al., 1999; Chuang et al., 2009; Li et al., 2014).

Hence, thermal pollution is seen as a severe threat for ecological composition in coastal waters around the World, and their industrial use as cooling agent is identified as its main cause.

Indeed, power plants typically use water from nearby bodies to cool their machinery, discharging it back at elevated temperatures, in a range of 5-100°C. Water used in industries for cooling purposes is released back to environment as thermal effluent; nuclear power plants require from 30% to 100% more cooling water rates than other types of plants of comparable power output, and their releases have been often investigated in terms of impacts on biodiversity (Li et al., 2014) and tourism development (Rosen et al., 2015).

Therefore, governments and international organizations set various standards regarding effluent temperatures from such facilities, in order to regulate their operation and minimize their environmental impacts (Manivanan and Singh, 2013). To address the impacts of thermal shocks on the aquatic environment, it is generally required to analyze the mechanism of dispersion of the thermal effluent in the water body nearfield of its release, and to establish a zone of influence where a certain temperature increment is acceptable.

Each EU-Country developed its own regulation regarding environmental standards for effluent temperatures in water bodies, implementing the specifics reported in the principal EU Directives, such as Water Framework, Habitats and Marine Strategy Framework Directives. A review of the regulations adopted by some EU Countries is listed in Appendix A.

Considering the above-depicted European framework, Italian regulation follows the general trend as far as both maximum effluent temperature and acceptable ambient-effluent temperature difference are concerned. D. Lgs. n.152 (2006) dictates that (i) the maximum water temperature at the outlet should not be higher than 35°C, and (ii) the maximum temperature increment in the coastal field, at a distance of 1 km from the outlet, should be lower than 3°C.

In temperate coastal and estuarine areas, cooling water discharge from power stations is typically between 8 and 12°C above the ambient water temperature, and recirculation of effluent water should be therefore granted by designing intake and outlet structures in order to allow a proper re-cooling of sea water (Durán-Colmenares, 2016).

The warmer water of the effluent is of course less dense than the receiving body water and therefore it tends to rise at the surface: a persistent interface is so generated because of this density difference, and dynamics like advection and diffusion tend to tone down such an interface, leading to complex mixing mechanisms. Depending on climate conditions, the environmental impact of thermal release into the sea can be more or less localized, and inducing some modifications in nearshore currents by power plant intake and thermal discharge systems (Elwany et al., 1990).

In addition, the diffusion of the cooling fluid in sea could also affect the efficiency of the heat exchangers of the power plants, since the inflow temperature (eventually influenced by the thermal outflow) should be taken into account during the design of the plant machines. More site-specific analysis on the developing thermal plume is then needed for multi-units at the same site to assure sufficient separation between the inflow and outflow waters, to be evaluated together with operational limitations due to the seawater temperature (Kim and Jeong, 2013).

Accordingly, the estimation of the mixing area (or thermal plume) seems to be critical to ensure compliance with the National regulation limits, and is largely influenced by parameters such as outflow discharge and velocity, cooling water temperature, and sea and coastal ambient conditions (SST, currents, tides, wave and wind regimes, infrastructures, economical facilities, etc.).

Furthermore, effects induced by the present climate variability and the expected climate changes should not be neglected, considering the dire consequences those already have/will have on mean sea temperature (Schaltout and Omstedt, 2014), along with the design life time of power plants (exceeding 30-50 years in most cases).

The present study focuses on dynamics induced by thermal discharge release in the coastal area of Cerano, South Italy, in the vicinity of a power plant, which uses seawater as a cooling agent. The investigation is carried out by means of a coupled wave - 3D-hydrodynamics numerical model TELEMAC, and the paper is organized as described in the following.

Section 2 presents the state-of-the art in the numerical modelling of coastal water quality, with a focus on thermal discharge. The case study of Cerano is described in Section 3 where site characteristics, collected field data to implement and verify the model and numerical setup are illustrated. Section 4 presents the model calibration and sensitivity analysis specifics, discussing in detail all data and model parameters involved, by means of typical performance indices. Results of the calibrated model runs are shown in Section 5 for the 3 hypothetical representative scenarios of environmental and operational conditions, namely: SC1, focusing on tidal and wave conditions; SC2, focusing on water temperature stratification in the coastal field; and SC3, focusing on the operational characteristics of the power plant (i.e., water discharge and effluent temperature).

The presented numerical investigation is the first authors' step towards the better understanding of thermal discharge dynamics in coastal areas, by means of numerical modelling of thermal pollution. Furthermore, the study is among the few in relevant literature that focuses directly on thermal discharge dynamics rather than studying it indirectly through its biological impacts, and is deemed to set the bases for future work on the same path.

2. Modelling coastal water quality with focus on thermal discharge: a state-of-the-art

As also mentioned in the previous, coastal water quality is essential for the preservation coastal ecosystems and the sustainable evolution of human activities in coastal and marine areas. As such, it has been extensively studied over the years by various means, ranging from simple observational and monitoring techniques to entire frameworks, and from simple empirical equations to entire computational systems. Given the advances in computational power nowadays, numerical modelling has become the main tool for the investigation of the effects that various natural and/or human forcings have on water quality, by being able to: (i) incorporate the representation of a wide array of processes and interactions, and (ii) examine multiple scenarios of the aforementioned forcings for research and operational purposes. In the following, the theoretical background and advances in coastal water quality modelling is presented, with a clear focus on thermal discharges in coastal/marine waters.

Regarding natural forcings, the ones referred to as "metocean forcings" are quintessential for coastal water quality modelling, comprising wind, air temperature, humidity, precipitation, etc. Accurate meteorological data are required at the water surface to act as boundary conditions (James, 2002), driving the currents through wind stress, changing the temperature through heat fluxes and salinity through precipitation and evaporation. Wave effects are important in the surface layer and in shallow water, where coupled wave-hydrodynamics modelling is required in order to account for increased mixing due to breaking waves and wave-induced enhancement of bed stress. In addition, wave-driven residual flows (such as Stokes drift and longshore currents) are particularly important when studying thermal discharge in coastal areas, with the second ones constituting probably the strongest drive for thermal plumes within the breaker zone.

Regarding human forcings, one may refer – in general – to the addition of pollutants and/or contaminants to the coastal/marine environment that deteriorate water quality (sediments, metals, oil spills, chemicals, toxins, thermal discharges, plastics, etc.), as results of various economical and recreational man activities. Focusing on thermal discharge studies – and in the context of this work – a basic division can be made into: (i) studies that examine the problem indirectly, though its biological impact on coastal ecosystems, and (ii) studies that examine the direct effects of thermal discharge on water temperature (SST distribution, depth stratification) and local hydrodynamics. The second ones, when based on numerical modelling like the present work, offer a better understanding of the actual processes involved in the studied phenomena and are more versatile, in the sense that they can be used both for quantitative comparative evaluations and as bases for other studies on the indirect effects of thermal pollution.

Falling into the first of the above categories, one could refer (indicatively but not exclusively) to the works of: Chuang et al. (2009), who studied the effects of elevated water temperatures and residual chlorine from thermal discharge by a coastal nuclear power plant in Taiwan on aquatic flora characteristics; Ingleton and McMinn (2012), who proposed a multidisciplinary approach for assessing effects of thermal pollution on estuaries based on biotic indices and satellite observations; Lardicci et al. (1999) and Li et al. (2014), who studied the impact of thermal discharge on benthic communities based on field measurements and statistical analyses; and Poornima et al. (2005), who studied the impact of thermal effluents from a coastal power plant in India on phytoplankton based on field observations and laboratory experiments.

Regarding studies falling into the second category, one could start from the ones utilizing field measurements and observational data, referring to the works of: Elwany et al. (1990), who studied the modification of coastal currents by a power plant's intake and thermal discharge systems in Southern California based on current measurements, trajectory experiments and their statistical analyses; and Muthulakshmi et al. (2013), who studied the plume dispersion from the thermal outfall of a nuclear power in India using thermal infrared images along with field measurements. Moving forward, works on the bridging of near- and far- field analysis are also worth mentioning, with the work of Israelsson et al. (2006) and Suh (2001, 2006, 2014) standing out in relevant literature. Israelsson et al. (2006) proposed the use of Lagrangian approaches – independently or along Eulerian models – in order to extend the domain of near field analysis of contaminant mixing near pollution sources in inland/coastal water bodies, while Suh (2001, 2006, 2014) proposed a hybrid technique to simulate the dispersion of heat from thermal discharges combining near-field models (e.g., CORMIX and ADCIRC) and far-field Eulerian-Lagrangian transport models.

Although the above constitute valuable background knowledge for researchers working on such relevant phenomena, studies on the numerical modelling of thermal discharge are the most essential for research and operational purposes nowadays, and helped formulate the study design and realization of this work as well. Listing a number of different modelling approaches used for the simulation of temperature and hydrodynamics evolutions due to thermal discharge, one could refer to the works of: Wu et al. (2001), who applied the 3D hydrodynamic and transport model GLLVHT (Generalized Longitudinal-Lateral-Vertical Hydrodynamic and Transport; Edinger and Buchak, 1980); Schreiner et al. (2002), who put in test the Cornell Mixing Zone Expert System (CORMIX, Jirka et al., 1996); Kolluru et al. (2003), who used the Generalized Environmental Modelling System for Surface Waters (GEMSS) and a probabilistic approach for the definition of the discharge's mixing zone; Chen et al. (2003), who used the 3D Finite Volume Coastal Ocean Model (FVCOM); Maderich et al. (2008), who used the 3D numerical model they developed, named THREETOX; and Cardoso-Mohedano et al. (2015), who used the Stony Brook Parallel Ocean Model presented by Jordi and Wang (2012).

Indicative studies on the comparative evaluation of different models include those of: Stamou and Nikiforakis (2013), who presented an integrated model for the simulation of thermal effluent discharges to coastal waters, consisting of the near field model CorJet and the far field model FLOW-3DL, and compared their results to predictions from the CORMIX model; and Tang et al. (2008), who developed 3D Reynolds-averaged Navier–Stokes model for the simulation of initial mixing in the near-field of thermal discharges, and tested it in various configurations comparing their results to the results of both CORMIX and Visual Plumes (Frick et al., 2003).

Finally, and due to its connection to the numerical tools used in this work, reference should also be made to the work of (i) Bedri et al. (2014), who used the 2D and 3D hydrodynamics modules of the TELEMAC suite (TELEMAC-2D and -3D, respectively) in combination to the environmental model SUBIEF-3D (Luck and Guesmia, 2002) in order to investigate the impact of a mixed sewage treatment plant and power plant effluence on coastal water quality and of (ii) Matta et al. (2017), who investigated the 3D flows induced by moderate or extreme winds in a Brazilian bay.

3. The case study of Cerano, South Italy

3.1 Site description

The study comprises the coastal area in the immediate vicinity of the ENEL Federico II power plant at Cerano, about 12 km south the city of Brindisi in South Italy (see Figure 1).

The coastline near Cerano is made up of cliffs with a very small sandy beach at the foot; the cliffs are made up of sandy-clayey soils, sometimes weakly cemented, however easily erodible by the aggression of the incident wave motion, with no beach at the foot along the northern sections of Cerano, and very small sandy strips along the southern slope (MATTM, 2017).

The coastline is under strong erosion due to the continuous dismantling action of the storms which, abrading the foot of the cliff's sides, establish precarious equilibrium conditions, which result in collapses and erosion tendency.

The substantial shoreline retreat has led over time to the construction of some coastal defense works. Already before 1992, the littoral stretch south the plant had been protected by a revetment made from natural boulders, and, some years later, rubble-mound emerged breakwaters and groins were constructed along the coast, inducing modifications in the sediment transport of the area. Indeed, breakwaters induced a considerable accumulation of sediment over the years in the area protected by the cliffs, leading to the formation of typical tombolos, while groins trapped sand on their north side, but caused beach erosion on the south side of the structures, due to the prevailing direction of the solid longitudinal transport from north to south.

The wave data collected in the period 1989-2012 by the RON - Italian Data Buoy Network (Franco and Archetti, 1993; Franco, 1995; Archetti et al., 2016) buoy placed offshore Monopoli, around 70 km north the study site, are analytically transposed offshore the study site, according to the geographic fetch-based approach (Contini and De Girolamo, 1998). Therefore, the reconstructed typical wave climate at Cerano is found to be characterized by NNW and ESE storms, mainly generated by Mistral (cold and dry wind usually blowing during the winter) and by Sirocco (warm and humid wind, generally inducing high storm surge), respectively.

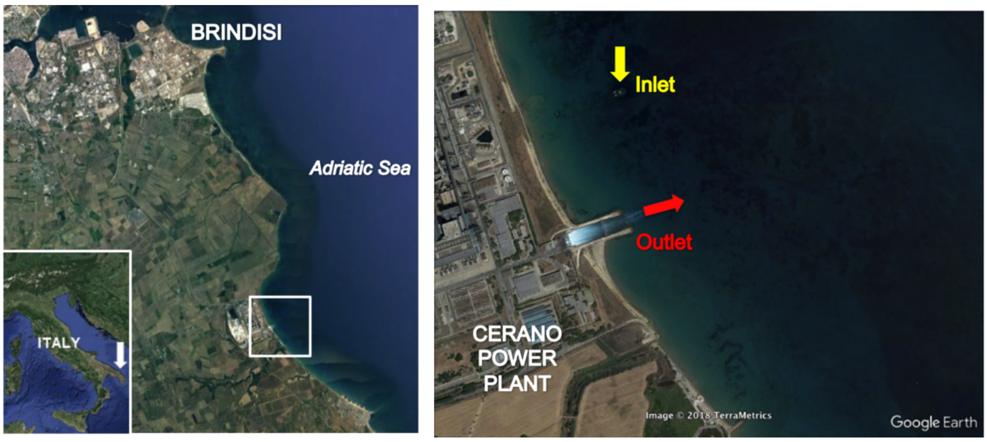

Figure 1. Satellite view of the studied area of Cerano (Italy) from Google Earth, 2018 (left panel) and a zoomed view on the area of the cooling water release (right panel).

In the study site, the net annual longshore sediment transport is directed from NW to SE, according to the Italian Atlas of beaches (1997), while sediment exchange with nearby coastal areas is limited/constrained by the headland located at the north, i.e. south of Brindisi (Delle Rose, 2015).

Covering an area of about 270 hectares and with a total installed capacity of 2640 MW, the thermoelectric (coal) power plant "Federico II" is one of the largest in Europe, with an electrical mean efficiency estimated to be of 35.6 % in the period 2003-2006 (Environmental Declaration – Enel Production, 2012).
Seawater is withdrawn at around 300 m from the shoreline and at a water depth of 5 m, with an inlet system of four pipelines. Heat exchangers are cooled by this sea water transported by a single pump of 1.000 m^3/h capacity and, at the end of the production cycle, the cooling fluid comes back to sea thought a discharge channel with an outlet width of 80 m, reaching a total estimated outflow of 3 bn. tons of water per year, corresponding to an annual average rate of 100 m^3/s (Environmental Declaration – Enel Production, 2012). Based on the plant's design conditions, the maximum temperature difference between inflow and outflow waters is therefore estimated to be set to 12 °C.

3.2 Field data

Instantaneous values of conductivity, temperature and density (CTD) have been provided by the environmental agency of the Apulia Region – ARPA - regarding a monitoring campaign carried out on the day 17 July 2002. During this campaign, CTD profiles were obtained at 23 points in the sea offshore the Cerano power plant, as presented in Figure 2; the geographical coordinates (East, North) of the measurement points together to the values of the depth-average temperature and standard deviation are listed in Table 1.

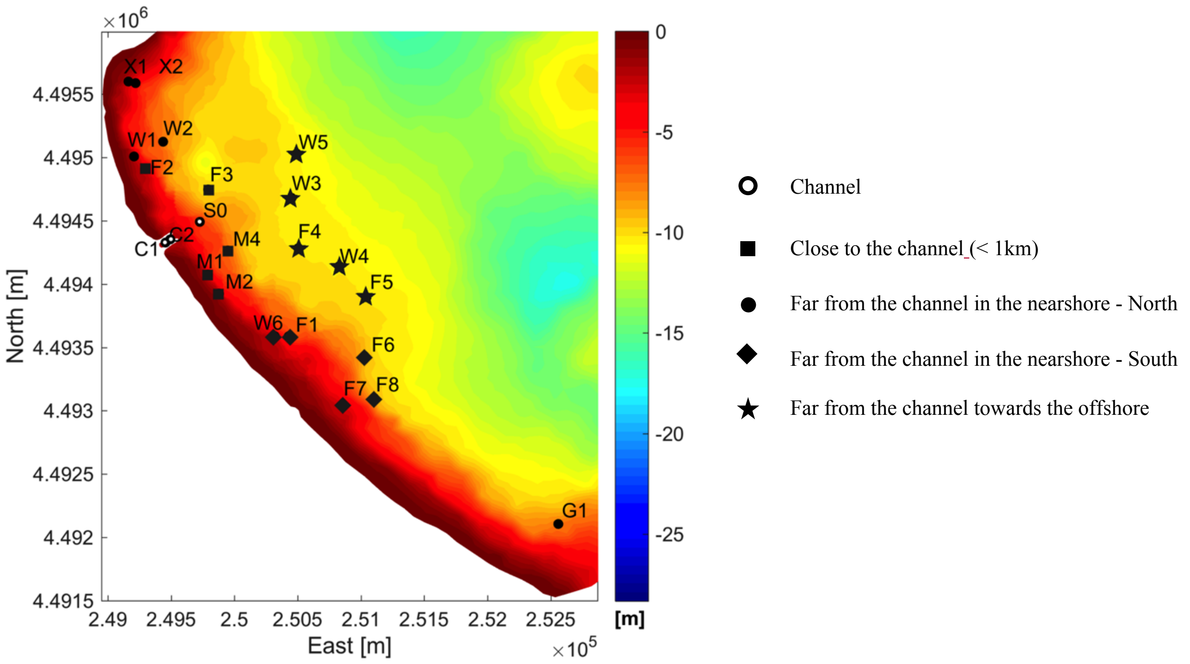

Figure 2. Positions of the 23 points of CTD measurement and legend of their symbols according to the location group in Table 1.

Due to the spatial distribution of the measurement points, the dataset is divided into 5 categories (reported in the last column of the table) in relation to the distance from the outlet channel and the shoreline. Classes are: “Channel”, including the 3 points located inside outlet channel; “Close to the channel (< 1 km)”, including points at a distance less than 1 km from the channel; “Far from the channel in the nearshore - North” and “Far from the channel in the nearshore - South”, including points close to the shoreline (water depth < 5 m) and located at north and south of the channel, respectively; and finally, “Far from the channel towards the offshore”, including points offshore (water depth > 5 m).

Table 1. Locations of the ARPA-Apulia points where CTD measurements were collected, depth-average temperature and standard deviation and their location group in the area.

Points ID	East [m]	North [m]	Depth-average temperature [°C]	Std Temperature [°C]	Location group
C1	249456.3	4494329.5	35.4	0.02	Channel
C2	249494.0	4494353.0	33.7	2.12	
S0	249726.0	4494492.0	31.6	0.83	
F2	249293.8	4494909.5	26	0.45	Close to the channel (< 1km)
F3	249792.6	4494748.5	25.8	0.54	
M1	249789.3	4494075.5	26.5	0.67	
M2	249877.1	4493926.5	28.3	0.72	
M4	249947.9	4494264.0	25.8	0.43	
X1	249164.3	4495601.0	26.5	0.79	Far from the channel in the nearshore - North
X2	249219.6	4495588.5	26.4	0.70	
W1	249206.3	4495009.0	26	0.48	
W2	249437.0	4495125.5	25.9	0.57	
F1	250430.3	4493587.5	26.8	0.64	Far from the channel in the nearshore - South
W6	250318.6	4493590.0	27.8	0.32	
F6	251028.7	4493431.0	26.1	0.64	
F7	250859.6	4493046.0	27.1	0.64	
F8	251102.7	4493102.0	26.6	0.54	
G1	252558.3	4492106.5	26.4	0.51	
F4	250503.6	4494285.0	26.3	1.09	Far from the channel towards the offshore
F5	251044.4	4493898.0	26.1	0.75	
W3	250451.9	4494679.5	25.5	0.46	
W4	250830.0	4494141.5	26.2	0.71	
W5	250490.9	4495030.0	25.6	0.55	

Waves were acquired from RON at the Monopoli buoy and propagated at the offshore boundary of study site, wind time series have been retrieved from the Italian National Tide Gauge Network (RMN), while the global database TPXO (Egbert and Erofeeva, 2002) was used for tides.

3.3 Numerical modelling

Approaching the coastal region, waves generated offshore are influenced by shoaling, refraction, and loss of energy either due to bottom friction and wave breaking (Buccino et al., 2014; Cavaleri et al., 2018). To simulate all these physical processes, including wave-induced currents, the present study of thermal discharge dispersion to the coastal area of Cerano is carried out using the numerical modules of the TELEMAC-MASCARET suite (available at TELEMAC, 2018) that is distributed under a General Public License.

The suite comprises finite-element-based solvers to simulate shallow water hydrodynamics and wave propagation, and is able to model inshore water levels and wave spectra under different drivers. The different modules comprised in the suite can simulate wind wave propagation, ground water flows, tracer transport, sediment transport, and morphodynamics.

The wave and 3D hydrodynamics modules of TELEMAC-MASCARET suite are TOMAWAC and TELEMAC3D, respectively and they were implemented in the proposed approach in order to propagate offshore waves and currents and reproduce nearshore dynamics influencing the thermal release at Cerano.

TOMAWAC module (henceforth denoted as TOM; Benoit et al., 1996) solves a simplified equation for the spectro-angular density of wave action by means of a finite-element type method (Booij et al., 1999), in order to describe wave propagation and dynamics in coastal areas. This module is properly set up for the studied area based on previous experience on coupled wave–2D hydrodynamics runs for the representation of nearshore processes, as presented in Samaras et al. (2016), Gaeta et al. (2016) and Gaeta et al. (2018).

The processes included in the wave model simulations are: (i) energy dissipation due to wave breaking according to Battjes and Janssen (1978), (ii) energy dissipation due to bottom friction according to Hasselmann et al. (1973), and (iii) nonlinear transfer of energy due to triad (three-wave) interactions according to Eldeberky and Battjes (1995). No movable seabed, no defense breaching, and no past subsidence-induced movements were assumed in the study.

The 3-D Navier–Stokes equations are solved in TELEMAC-3D (henceforth denoted as TEL3D; Hervouet, 2007), with the option of the non-hydrostatic pressure hypothesis, and includes: (i) the use of a finite element unstructured grid, which allows selective refinement of the mesh at key locations in the domain and boundary fitting method for vertical discretization; (ii) the transport-diffusion equations of intrinsic quantities (temperature, salinity, concentration), in order to reproduce 3-D hydrodynamics including the trans- port of active and passive tracers; (iii) a wide range of options for vertical turbulence modelling.

The governing equation of the tracer transport is reported in Equation (1), as:

$$\frac{\partial(\rho T)}{\partial t} + u\frac{\partial(\rho T)}{\partial x} + v\frac{\partial(\rho T)}{\partial y} + w\frac{\partial(\rho T)}{\partial z} = U_x\frac{\partial(\rho T)}{\partial x} + U_y\frac{\partial(\rho T)}{\partial y} + U_z\frac{\partial(\rho T)}{\partial z} \quad (1)$$

where T and ρ represent the water temperature and the water density, respectively; u, v and w are the water velocity components and U_x, U_y and U_z are the turbulent thermal diffusivity components along the *x*, *y* and *z* the spatial coordinate system, respectively; *t* is time.

The latest release of TELEMAC (version 7.0) includes the implementation in TEL3D of thermal exchange fluxes between sea and atmosphere, including typical processes of net solar radiation (Cooper, 1969), long-wave radiation (Berliand and Berliand, 1952), sensible heat (Rosati and Miyakoda, 1988) and latent heat due to evaporation (Panin and Brezgunov, 2006).

TEL3D can be directly coupled (two-way coupling) with the spectral module TOM on the same computational mesh in order to reproduce the dynamics of wave-driven currents; the gradients of the radiation stress induced by waves are computed using the theory of Longuet-Higgins and Steward (1964) as part of the hydrodynamics equations. The updated values of current velocities and water depths calculated in TEL3D are transferred to TOM, while TOM solves the wave action density conservation equation, and returns the updated values of the wave driving forces acting on the current to the hydrodynamics modules (Hervouet, 2007).

The initialization strategy of the implemented high-resolution model followed the methodology described in Federico et al. (2017), where initial condition fields on temperature were provided by the Mediterranean Forecasting System MFS (produced by data assimilation), which supplies operational forecasting products in the framework of CMEMS (Copernicus Marine Environmental Monitoring Service, available at http://marine.copernicus.eu/). Figure 3 shows the sea temperature field at day 17 July 2002, as obtained by MFS, and the profiles at 4 selected nodes, the ones falling into the study area and therefore used to set initial conditions of the present implemented model.

According to the experience and validation shown at large and coastal scale (Cucco et al., 2012; Trotta et al., 2016) and at harbor scale (Gaeta et al., 2016), a spin-up time of 3 days was considered to be a reasonable choice in order to ensure the development of internal dynamics by the nested model. Therefore simulations were carried out for the period between 14 and 17 July 2002, that is the day when measurements were collected.

Interpolating the oceanic fields over the new higher-resolution grid is solved following the procedure suggested in De Dominicis et al. (2013) and validated in Samaras et al. (2014), although the local effects on sea temperature and hydrodynamics field induced by the cooling discharge from the plant are not captured in the MFS model, due both to its large mesh resolution (7 x 7 km^2) and the absence of any imposed liquid conditions at the shoreline boundary (no run-off and release into coastal waters).

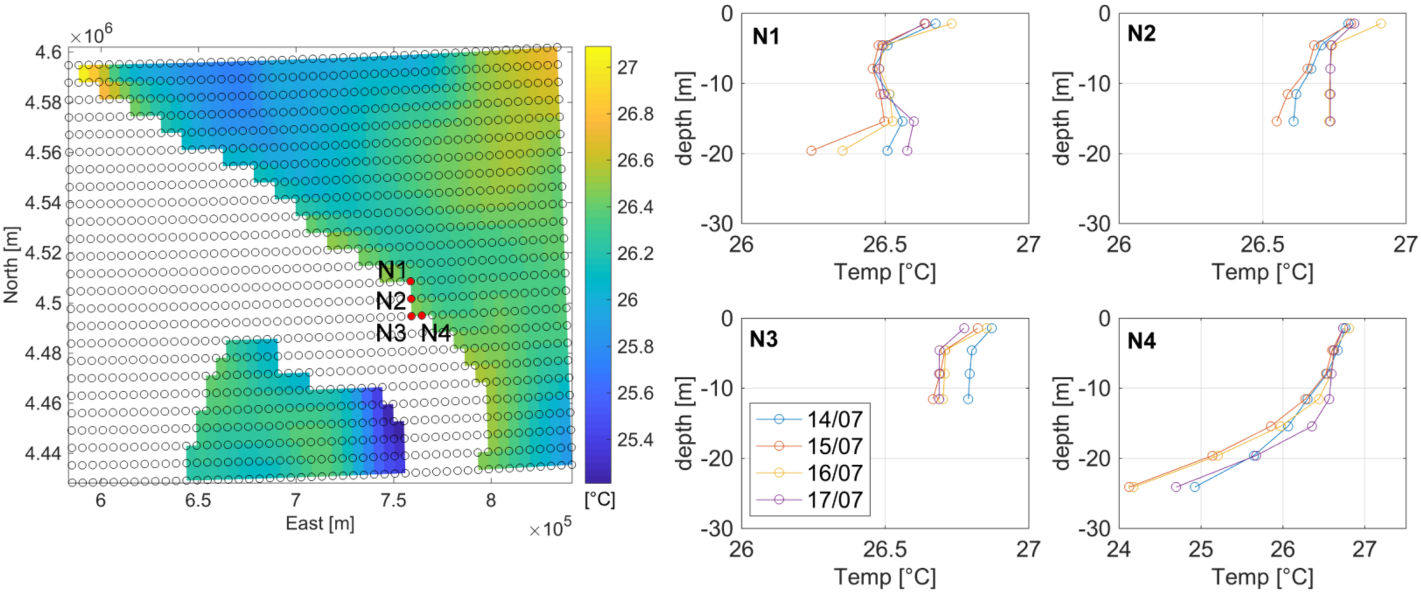

Figure 3. Sea surface temperature on 17 July 2002 extracted by Copernicus Service data (left panel) and daily average temperature profiles for the period 14-17 July 2002, at the 4 MFS nodes (right panels).

Details of the drivers used for the model runs are listed in Table 2, describing the initial conditions (IC), offshore boundary conditions (OBC), surface conditions (SC) and the imposed conditions at the channel (Outlet) of the modelled variables in TEL3D and in TOM, following the implemented multiple nesting procedure (Gaeta et al., 2016).

Table 2. Initial (IC), offshore boundary (OBC), surface (SC) and outlet conditions for the different modelled drivers

	Tide	Current	Wind	Wave(*)	Sea Temperature	Meteorological variables
IC	Null	Null	Null	Null	MFS	Null
OBC	TPXO	Null	-	Transposed RON	MFS	-
SC	-	-	RMN	-	-	RMN
Outlet	TPXO	Outflow (discharge constraint)	-	Open flow	Outflow	-

(*) Significant wave height, peak period and mean direction defining a JONSWAP spectrum in TOM.

In the model, finite element techniques were used to solve the hydrodynamic equations, adopting the z-vertical discretization to follow the surface and lower boundaries. The Multidimensional Upwind Residual Distribution method was applied for the advection of three-dimensional variables under TEL3D, and the boundary conditions were applied following the method of characteristics.

The advection of tracers was solved using the distributive MURD + PSI method and the prescription of tracers at the open channel was applied using imposition by the Dirichlet boundary condition, while a Neumann type condition at the offshore was prescribed, imposing a zero gradient of temperature.

The mesh for the implementation of the models in this work was generated using the freely-available pre-processing tool Blue Kenue (CHC, 2010). A series of tests proceeded the final mesh generation, in order to evaluate optimal mesh edge-dimension, in terms of both representing the processes of interest satisfactorily and keeping computational times to reasonable levels.

The selected variable density unstructured mesh (see Figure 4), consisted of two density regions: a coarse one (100 m edge length), extending from the offshore boundary and up to the plant outflow area, and a fine one (10 m edge length) in the immediate vicinity of the plant outlet and the nearby area, aiming to better capture the mixing dynamics following the thermal release. The number of nodes in the mesh equals to around 14.000.

The used bathymetric and shoreline data were obtained by digitizing nautical charts acquired from the Italian National Hydrographic Military Service (Figure 4). The resulting map clearly indicates a gradually changing bathymetric pattern moving offshore. In particular: depths (in the range of 2 - 3 m right in front of the shoreline) remain respectively low up to 500 m to the offshore, followed by the central mesh area which is characterized by depths ranging from 12 m to 18 m, eventually transitioning to depth reaching around 30 m near the offshore boundary of the modelled region (i.e., the boundary where waves are generated as well).

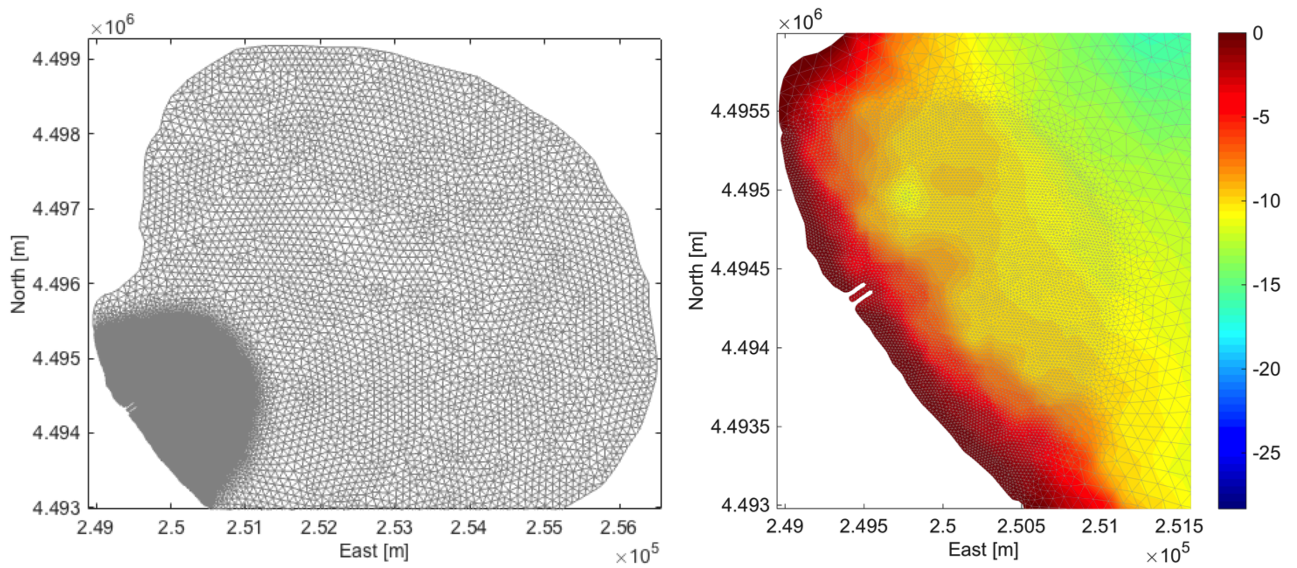

Figure 4. Mesh of the studied area (left panel) and a zoomed view of the interpolated bathymetry (right panel).

4. Model calibration and discussion

4.1 Sensitivity analysis on hydrodynamics drivers

A sensitivity analysis was performed on hydrodynamics drivers included in the simulations, in order to define which of them mostly influenced models performance, as being sensitive to the variation of the simulated processes. The analysis was carried out at the 7 points of the ARPA-Apulia measuring campaign, namely F2, F3, M1 – close to the outlet channel; X2, W6 – far from the channel in the nearshore – North and

South, respectively; W3 and F4 – far from the channel towards the offshore. These points were selected among the measurements as they are representative of the defined location groups (Table 1).

The analysis was applied to different drivers included in the simulations, as listed in Table 3, accounting for wave propagation (W), tidal elevation (T) and wind forcing (U), for a total of 8 performed runs.

Table 3. Modelled hydrodynamics drivers: wave (W), tide (T) and wind (U).

		Modelled process		
#	**Run name**	**Wave**	**Tide**	**Wind**
0	W0T0U0	-	-	-
1	W1T0U0	X	-	-
2	W0T1U0	-	X	-
3	W0T0U1	-	-	X
4	W1T1U0	X	X	
5	W1T0U1	X	-	X
6	W0T1U1	-	X	X
7	W1T1U1	X	X	X

To investigate the model performance, the Root Mean Square Error (RMSE) was evaluated allowing a comparison between the measured and the simulated temperature values. These parameters were calculated by using the expression:

$$RMSE = \sqrt{\frac{\sum_1^N (T_s - T_m)^2}{N}} \quad (2)$$

where N is the total number of the measured points (Table 1) along the collected vertical profiles, the index s is for the simulated value and m for the measured CTD data.

For each of the performed simulations, default values as defined by Hervouet (2007), Samaras et al. (2016) and Gaeta et al. (2016) were kept constant, as well as the number of horizontal layers (equal to 5).

Figure 5 presents the results of the sensitivity analysis in terms of RMSE for temperature values. The influence of the simulated processes strongly depends on the investigated location's distance from thermal discharge release point, with minimum errors resulting when all drivers were included in the run, i.e. W1T1U1.

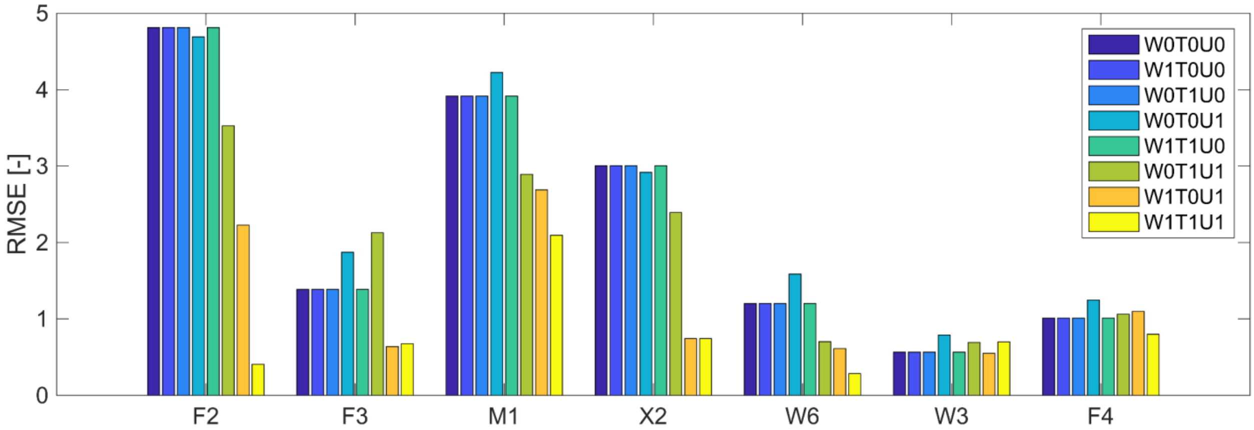

Figure 5. RMSE at different measured points: sensitivity analysis on the included simulated processes, as listed in Table 3.

In particular, points located close the channel, F2 - M1, present the highest errors – (ranging between 2 and 5) when waves and wind were excluded by the simulations, that were reported as crucial drivers to simulate the thermal diffusion in nearshore areas.

Therefore, coupling wave and wind modelling, despite rising the computational time by a factor 10, improves the quality of the results and might be accounted for in these complex coastal processes.

4.2 Sensitivity analysis on governing equations' parameters

A significant array of simulations was run in order to get a proper calibration of the models used in this work, on the basis of the available temperature profiles provided by ARPA-Apulia, by means of investigating the influence of the TEL3D parameters in order to reach the better agreement between data and simulations.

For the local sensitivity analysis, the performed simulations were carried out using the "one-at-the-time" approach (Simmons et al., 2015), by increasing each parameter by a given percentage while leaving all others constant, and quantifying the change in model output.

The parameters identified for the analysis characterize the processes involved in coastal thermal pollution, such as the number of the horizontal layers, the friction bottom coefficient, the horizontal and vertical turbulence models, the diffusion coefficients for velocity, the horizontal diffusion for temperature, and wind drag coefficient. All the other parameters, mainly regarding wave propagation and wave-current interactions, were kept equal to the calibrated values as defined by Hervouet (2007), Samaras et al. (2016) and Gaeta et al. (2016).

Table 4 shows the list of analysed parameters, their tested range and their corresponding final values adopted for the calibrated model runs. For this analysis, the physical processes by coupled wave -3D hydrodynamics modelling, including wind influence, were simulated according to the results shown in the global sensitivity analysis presented in the previous section.

Table 4. List of the parameters in TEL3D tuned in the sensitivity analysis (run W1T1U1).

Variable name	Variable description	Value range	Final value
nz	NUMBER OF HORIZONTAL LAYERS [-]	5 - 10	5
fs	FRICTION COEFF. FOR THE BOTTOM [$m^{1/3}/s$]	60 - 100	80
Tx	COEFFICIENT FOR HORIZONTAL DIFFUSION OF TRACERS [m^2/s]	10^{-6}- 10^{-1}	10^{-6}
Uz	COEFFICIENT FOR VERTICAL DIFFUSION OF VELOCITIES [m^2/s]	10^{-6}- 10^{-1}	10^{-6}
Ux	COEFFICIENT FOR HORIZONTAL DIFFUSION OF VELOCITIES [m^2/s]	10^{-6}- 10^{-1}	10^{-1}
kv	VERTICAL TURBULENCE MODEL	2 - 5 [a]	2
ml	MIXING LENGTH SCALE [m]	2 - 5	5
kh	HORIZONTAL TURBOLENCE MODEL	2 - 4 [a]	4
cd	COEFF. OF WIND INFLUENCE [m^3/kg]	2 - 10 x 10^{-3}	5 x10^{-3}

[a] 1= constant viscosity; 2=mixing length; 3= Prandt; 4=Smagorinsky; 5=k-ε

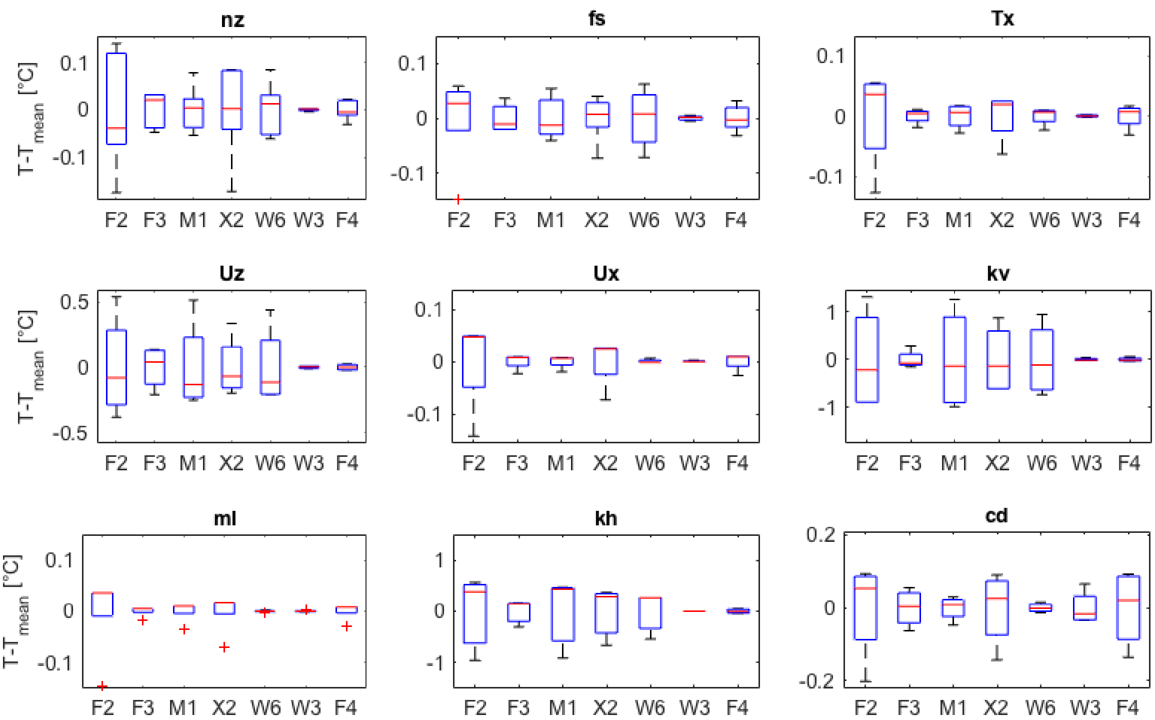

Figure 6. Results of the sensitivity analysis for each analyzed parameters in TEL3D for the 7 selected points.

Results of the 45 runs were summarized for the 7 selected measurement locations in Figure 6, where each panel shows the differences in depth-average temperature between measurements and model results for each of the 9 investigated parameters. In Figure 6, red lines represent mean values, top and bottom box edges represent the 75th and 25th percentiles, line limits represent maximum and minimum values, and red crosses indicate outliers.

The results show that the parameters that mainly influence the model quality, thus improving the numerical reproduction of the thermal mixing processes, are the choice of the vertical and horizontal turbulence models (kv, kh), the vertical diffusion coefficient (Uz), and the wind drag coefficient (cd).

The model sensitivity to the adopted turbulence models and velocity diffusivity appears to decrease with the increase of distance from the shoreline and from the release channel: points F2, F3 M1, X2 and W6 present the greatest variance in the agreement with measured temperatures. The influence of the drag coefficient for wind appears, on the other hand, to be spatially uniform ranging from -0.2 to 0.1.

Following the analysis on the parameters, the model can be assessed as calibrated, with reference to the thermal dynamics and climate of the study area.

4.3 Discussion on the numerical results from the calibrated model

Results of the final calibrated model as obtained after the sensitivity analysis, i.e. run W1T1U1, are presented in Figure 7, where temperature profiles at the 7 reference points analysed in the previous sub-sections were extracted from the numerical simulation and compared to the measurements.

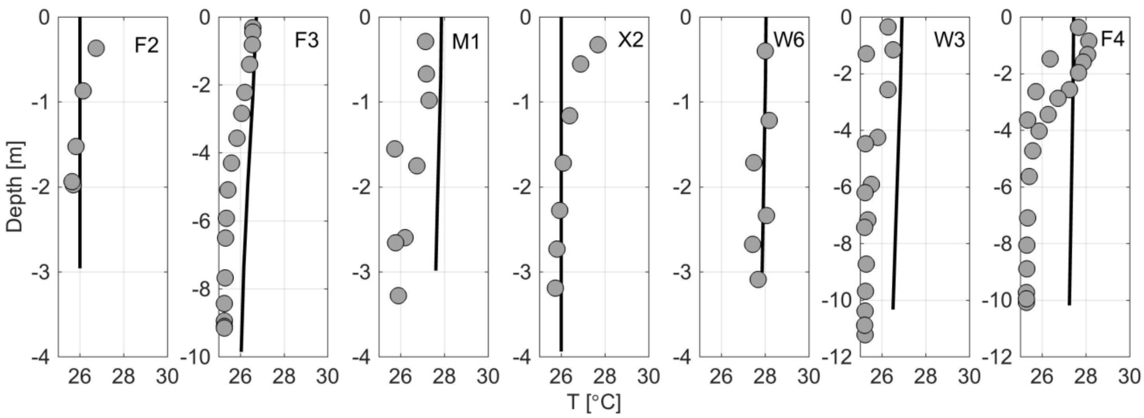

Figure 7. Comparison of temperature profiles: calibrated simulation (solid lines) and ARPA-Apulia measured data (points).

Although some uncertainties are present in the present numerical study about initial and boundary conditions implemented in the simulations, the calibration results in a satisfactory agreement to data, especially considering the complexity of the studied phenomenon, as well as the equally complex dynamics of the various processes' interactions involved in its numerical simulation. In particular, regarding the depth-average temperature, the following convergence results are observed: maximum deviation from data reaching +2 °C in just 2 of the examined locations; deviation less than +1 °C for 19 points; maximum deviation of +0.2 °C achieved for 6 out of the 23 examined points.

The greater difference is observed at points located offshore, i.e. W3 and F4, where the low temperatures (around 25°C) are not captured well by the model, overestimating them for water depths > 3 m. This can be attributed to the initial conditions used, as temperatures extracted by MFS are overall bigger than 26°C (see Fig. 3).

The temperature increment ΔT due to the power plant release with respect to the ambient values is shown in Figure 8, where the evolution of the plume development as discretized at the 23 points of the ARPA-Apulia campaign is shown the model results and the measured values, at a water depth equal to -1 m.

The overall diffusion of the thermal release is found to be well reproduced by the calibrated model, where the computed mixing area is slightly greater extending to the southern direction, revealing the flow directionality driven by wind and waves is satisfactory predicted in the simulation.

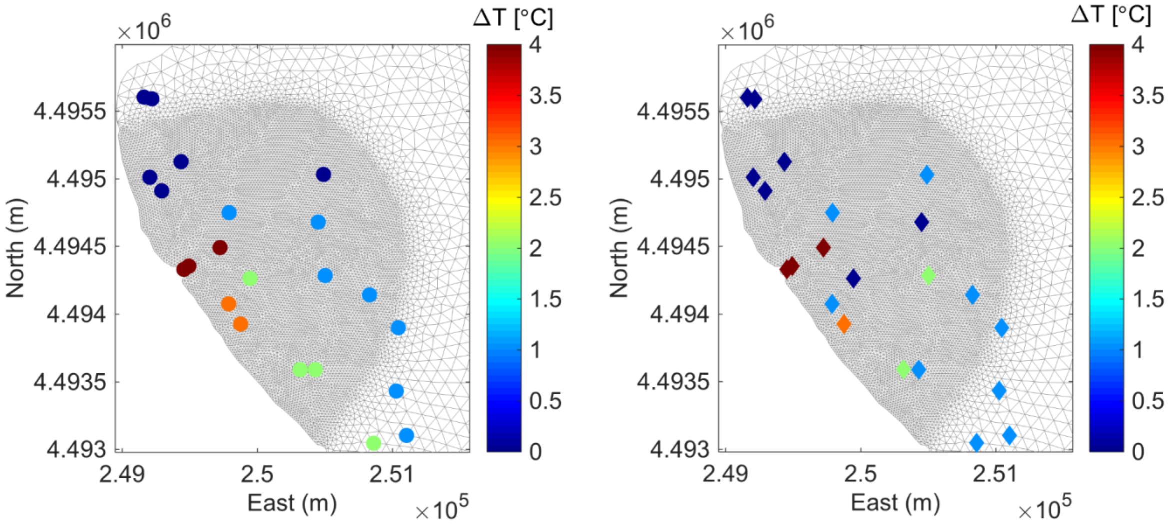

Figure 8. Numerical results (left panel) and measurements (right panel): temperature increment ΔT (colorbar) at a water depth equal to -1 m for the 23 points of the ARPA- Apulia campaign.

In accordance to the previous, Figure 9 shows the computed thermal plume in the studied coastal area, where the sea temperature at the end of the simulation reveals the prevalent dispersion of the cooling waters towards SSE and mainly along the southern shoreline. Arrows represent the velocity vectors: the prevalent longshore current is driven by wind and waves and directed from North to South with speed reaching up to about 0.20 m/s and that strongly affects the direction of the thermal plume. Both the presence of the two groins delimiting the outlet channel and the outflow speed of the cooling waters induce a perturbation in the actual current patterns, resulting in the development of: (i) a seaward directed plume, with a velocity of about 1 m/s and (ii) eddies downward the channel, eventually contributing to the observed shoreline retreat in this specific area. Under the simulated conditions, the directionality developed by the thermal plume is desirable in terms of power plant efficiency/performance, as the cooling waters move away from the morphologically-constrained area North of the channel (see also Figure 1), which could lead to its entrapment and consequent increment in local temperature, affecting both the water temperature at the intake (i.e., reducing the plant efficiency) and the acceptable thermal increment imposed by the National regulation.

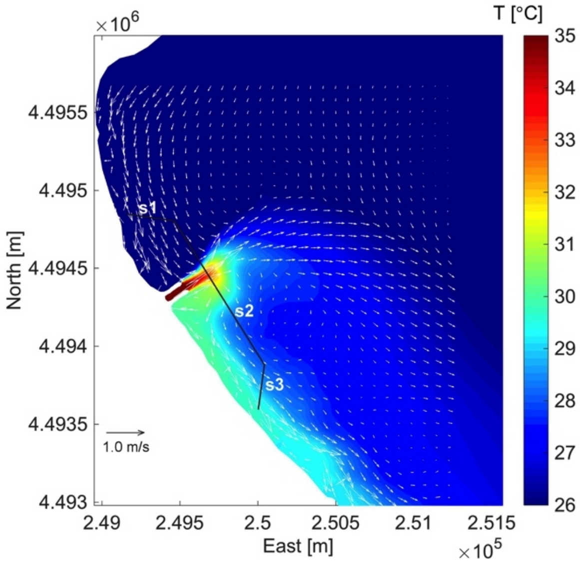

Figure 9. Sea temperature and velocity arrows, at water depth equal to -1 m, on the day 17 July 2002.

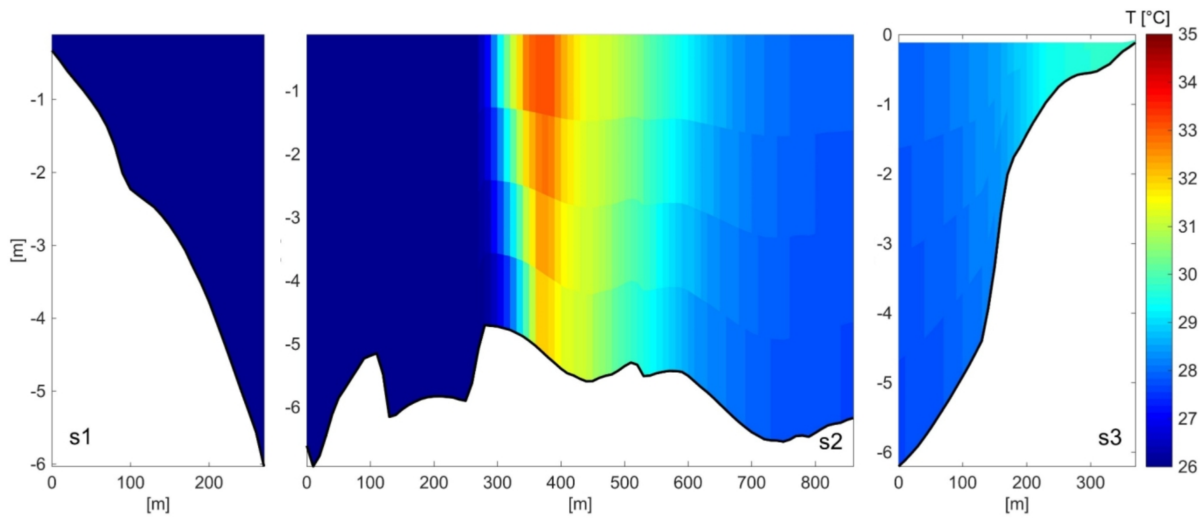

Figure 10. Vertical planes of the sea temperature along sections s1 (left panel), s2 (middle panel) and s3 (right panel), located as shown in Figure 9.

Figure 10 presents the sea temperature along the 3 selected planes, namely s1, s2 and s3, located at the vicinity of the release channel, as shown in Figure 9, for a water depth of around - 6 m (section s2, in the middle panel) up to the shoreline for sections s1 and s3 (left and right panels, respectively).

The presence of the cooling waters is clearly observed at the section s2 that is located just in front of the outlet, at a distance of around 100 m. There, the vertical gradient of the temperature slightly develops, probably due to the low wave intensity occurring during the simulated period. The horizontal dispersion of the thermal plume is observed as well, with temperature decreasing up of 6 °C along a 500 m long stretch. Results along section s3, instead, reveal high temperatures of around 30 °C at shallow waters (from depth of – 1 m up to shoreline), persisting along the 1-km long shoreline at the southeast of the outlet, as also represented in Figure 9.

5. Numerical experiments under different environmental and operational scenarios

After models' sensitivity analyses and calibration, a set of scenarios for different environmental and operational conditions were setup, so that a proper assessment of the cooling water release from the Cerano power plant could contribute towards: (i) implementing an effective monitoring program of the thermal plume, and (ii) establishing mitigation measures for its eventual environmental effects.

The aforementioned set of scenarios was setup in order to represent expected seasonal and industrial events, in order to test them against the "reference" scenario for the real on-site conditions, described in Section 4. This set, as listed in Table 5, comprised:

- SC1, representing the worst metocean conditions for dispersion, meaning no wind and therefore no waves, while maintaining the same operational features with the reference scenario;
- SC2, representing the maximum power production conditions of the plant (reference to data during the day 17 July 2002), with cooling waters at the outlet with a temperature of 35 °C and a temperature increment of 12 °C with respect to the ambient temperature, therefore set to be equal to 23 °C, while maintaining the metocean reference conditions;
- SC3, representing Sirocco conditions (i.e., overturning the wind and wave direction), while maintaining the same operational features with the reference scenario.

Table 5. Overview of the modified conditions for the simulated scenarios SC1, SC2 and SC3.

	Wind	**Wave**	**Temperature increment ΔT [°C]**
SC1	Null	Null	As in the reference scenario
SC2	As in the reference scenario	As in the reference scenario	Equal to 12°C
SC3	Direction from south to north	Direction from south to north	As in the reference scenario

Figure 11 illustrates the computed sea temperature field at a water depth of -1 m, at the end of each numerical experiment carried out for the period 14-17 July 2002, as in the reference scenario.

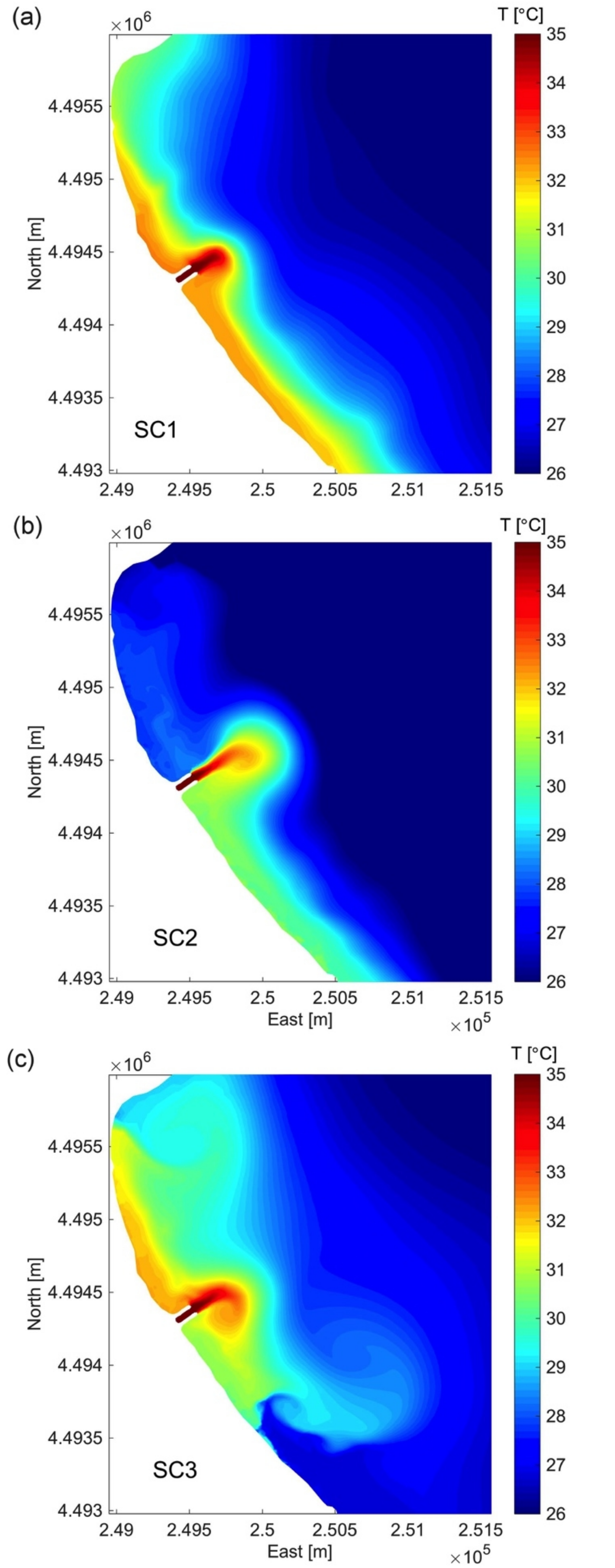

Figure 11. Sea temperature for the scenarios SC1 (panel a), SC2 (panel b) and SC3 (panel c).

For scenario SC1 (Figure 11a), the absence of any metocean forcings tends to make the thermal plume stay in the area, the temperature spread towards the south being lower than in the reference scenario (see Figure 9 for comparison). Furthermore, the plume is limited to the nearshore, spreading out in a similar way towards the areas located north and south of the outlet, consequently affecting the former one which was not polluted in the reference scenario. Scenario SC2 (see Figure 11b), is characterized by a thermal discharge with a temperature increment of 12 °C with respect to the ambient temperature and cooling waters at the outlet with a temperature of 35 °C. In comparison with the reference scenario (see Figure 9), SC2 results reveal a similar plume distribution pattern, although – as expected – a wider zone of influence was present, expanding northwards of the outlet as well (where impact was minimal in the reference scenario).

In SC3 (Figure 11c), the prevalent direction of the thermal plume propagation reverses from south-southeast to north-northwest, although evidence of spreading is observed north of the outlet as well. The Northern area (also mentioned in Subsection 4.3) constrains plume propagation and leads to thermal amassing in the area. In this scenario, the efficiency of the power plant is expected to be significantly affected, due to the dual effect of the water intake's location being in the area and the environmental implications of the temperature difference increase.

Following the analysis by Durán-Colmenares et al. (2016), the spatial decay of the depth-average temperature with respect to the ambient condition (T_0) was estimated along a cross-shore section starting at the outlet and extending up to 1500 m offshore, for all the 3 scenarios and the reference simulation (i.e., on the day 17 July 2002). The values of the decay, presented in Figure 12, were normalized with the maximum temperature value (T_{max}) at the outlet, changing with the simulated scenarios.

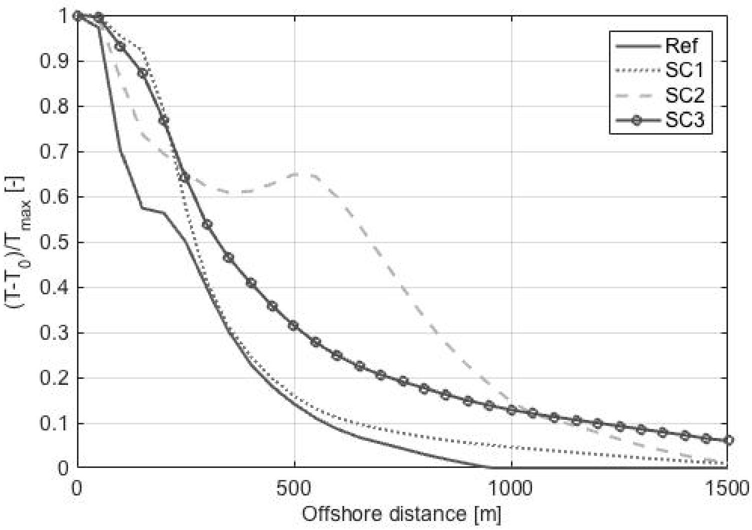

Figure 12. Temperature decay curves along the cross section from the channel for the reference and scenario simulations.

Along the analyzed cross-shore section, for the reference, SC1 and SC3 scenarios, the percentage of dissipated temperature decreases up to 50 % at a distance of around 300 m from the outlet, and arrives to be around null within 1000, 1500 and 1600 m respectively. The change of the metocean forcings in SC1 (null drivers) and SC3 (overturning drivers) is primarily responsible for the lower heat dispersion offshore in comparison to the reference conditions, while closer to the shoreline, the sea temperature increment remains fairly unaltered.

The variation of the industrial conditions in SC2, instead, has the main influence on heat dispersion into the sea, reducing the decay rate of the temperature towards the offshore.

The areas of influence for all scenarios (Table 6) were calculated for each simulation and per range of temperature increment, referring to the computed sea surface temperature. The values were normalized with the total volume of hot waters released by the power plant, since the industrial conditions varied between scenarios.

Table 6 Normalized areas of influence of the thermal plumes per range of temperature increment.

$T-T_0$ [° C]	Normalized area of influence [%]			
	Reference	**SC1**	**SC2**	**SC3**
> 8	0.2	0.3	1.5	0.3
> 7	0.3	0.7	6.0	0.7
> 5	0.6	11.0	17.0	7.2
> 3	7.5	30.0	41.0	30.3
> 1	51.0	97.0	69.0	94.0

Considering the geographical extent of the implemented numerical domain (Figure 4), wind from the north allows the greater rates of heat dispersion, mainly occurring towards the south (Figure 11) and giving up to 50% for a temperature increment less than 1 °C, while, still persisting the same metocean conditions, in SC2, areas of influence are greater, from 1.5 % for higher values (greater than 8 °C) up to 69 % for lower values of temperature (greater than 1 °C).

The maximum area of influence for lower temperature increments is then obtained for scenario SC1 (97 %), i.e., in absence of any metocean forcing, and for scenario SC3 (94 %), i.e. for the south wind, the case where the cooling waters would have difficulties to spread offshore (and outside the numerical domain) due to the northern coastal morphology (cove-like formation) of the area that leads to an eventual thermal amassing.

6. Conclusions

This work presents the setup, sensitivity analysis, calibration/validation and implementation of a coupled wave – 3D-hydrodynamics model for the investigation of thermal discharge dynamics in coastal areas. The model setup is based on the respective spectral and 3D-hydrodynamics modules of the open-source TELEMAC suite. The implemented case regards a thermal power plant in South Italy, which uses seawater intake for cooling purposes and releases hot water back to the sea through a coastal outlet. After an extended sensitivity analysis, the coupled model was calibrated by using the sea temperature data collected during the field campaign of ARPA-Apulia in the area.

Sensitivity analyses highlighted the importance – for model performance in the representation of thermal discharge to coastal areas – of: (i) wave – wind combination, regarding model drivers, and (ii) vertical/horizontal turbulence models, vertical diffusion coefficient and wind drag coefficient, regarding governing equations' parameters. Model calibration/validation is deemed to have been successful, managing to capture satisfactorily both the horizontal and vertical distribution of water temperature variations.

The final runs of the calibrated model regarded scenarios of environmental and operational conditions, in order to investigate representative "states" of the specific coastal system, in terms of both environmental issues (i.e., temperature increment in the nearshore area) and plant efficiency issues (i.e., performance related to inflow temperatures). The 3 simulated scenarios revealed the range of expected changes in the thermal plume's distribution for representative conditions in the field (environmental/operational), providing useful insights on the specific case study's dynamics.

All in all, the present work is among the relatively few in relevant literature that focuses directly on thermal discharge dynamics rather than studying it indirectly through its biological impacts and is deemed to constitute a useful basis for other studies on the topic, either direct or indirect. Future versions of this work could be further improved by investigating case studies with more extensive field measurement datasets (e.g., current/wind data) and/or coupling the wave and 3D-hydrodynamics modules with the water quality module of TELEMAC (available in the suite's last release), in order to extend this approach's applicability. Nonetheless, the systematic literature review, analysis of the studied phenomenon, and modelling approach followed in this work, contribute to setting the framework for the direct numerical simulation of thermal discharges to coastal areas, while also setting the bases for the specific case study's evaluation and environmental/technical assessment.

Acknowledgments

The authors would like to thank Mr. Ungaro from ARPA- Apulia for proving the CTD data of the field campaign in 2002. The research was partially funded within the framework of the Italian Flagship Project "TESSA – Development of Technologies for the Situational Sea Awareness" supported by the PON01_02823/2 "Ricerca & Competitività 2007–2013" program of the Italian Ministry for Education, University and Research.

Appendix A. Regulations in EU Countries for thermal release in coastal area

The principal EU Directives, such as Water Framework, Habitats and Marine Strategy Framework Directives, do not require a trans-European thermal standard, therefore each EU-Country developed its own regulation (British Energy Estuarine & Marine Studies March, 2011) regarding environmental standards for effluent temperatures in estuarine, coastal and marine systems, and in particular their allowed temperature values was here listed and reviewed:

• In France, on the Gironde Estuary, the temperature increment must be not greater than 11 °C at the outflow point, with a maximum temperature of 30 °C, with a permission to reach up to 36.5 °C in summer.

• In Norway, the temperature increment must be not exceeding 10 °C at the outflow point and no more than 1 °C of temperature increment in the mixing zone, with some flexibilities up to 3 °C at particular sites.

• In Spain, 50 m or more from the discharge point in any 1 m layer within the water column the temperature increment must not exceed 3 °C or 1 °C integrated throughout the water column.

• In Germany, maximum limit for cooling water discharges is at 30 °C and the temperature increment must be not exceeding 10 °C for existing sites, and 7 °C for a new plants.

• In the Netherlands, discharges into marine waters must not exceed 30 °C within a mixing zone bounded by the 25 °C isotherm.

• In Italy, the maximum water temperature at the outlet should not be higher than 35 °C and the maximum temperature increment in the coastal field, at a distance of 1 km from the outlet, should be lower than 3 °C.

References

Archetti, R., Paci, A., Carniel, S., Bonaldo, D., 2016. Optimal index related to the shoreline dynamics during a storm: The case of Jesolo beach. Natural Hazards and Earth System Sciences, 16(5), 1107-1122.

Azmi, S., Agarwadkar, Y., Bhattacharya, M., Apte, M., Inamdar, A.B., 2015. Monitoring and trend mapping of sea surface temperature (SST) from MODIS data: a case study of Mumbai coast. Environmental Monitoring and Assessment 187.

Battjes, J.A., Janssen, J.P.F.M., 1978. Energy loss and set-up due to breaking of random waves. In Proceedings of the 16th International Conference on Coastal Engineering, Hamburg, Germany, 27 August–3 September 1978; pp. 569–587.

Bedri, Z., Corkery, A., O'Sullivan, J.J., Alvarez, M.X., Erichsen, A.C., Deering, L.A., Demeter, K., O'Hare, G.M.P., Meijer, W.G., Masterson, B., 2014. An integrated catchment-coastal modelling system for real-time water quality forecasts, Environmental Modelling & Software 61, 458-476.

Benoit, M., Marcos, F., Becq, F., 1996. Development of a third generation shallow-water wave model with unstructured spatial meshing. Proc. 25th International Conference on Coastal Engineering, Orlando.

Berliand, M.E., Berliand, T.G., 1952. Measurements of the effective radiation of the Earth with varying cloud amounts. Izv. Akad. Nauk SSSR Ser. Geofiz., 1.

Bonaldo, D., Antonioli, F., Anzidei, M., Archetti, R., Bezzi, A., Correggiari, A., Davolio, S., De Falco, G., Fantini, M., Fontolan, G., Furlani, S., Gaeta, M.G., Leoni, G., Mastronuzzi, G., Pillon, S., Stocchi, P., Samaras, A.G., Carniel, S., 2018. Integrating multidisciplinary instruments for assessing coastal vulnerability to erosion and sea level rise: lessons and challenges from the Adriatic Sea, Italy. J. Coastal Conservation 23 (1), 19–37.

Booij, N., Ris, R.C., Holthuijsen, L.H., 1999. A third-generation wave model for coastal regions 1. Model description and validation. Journal of Geophysical Research 104 (C4), 7649–7666.

Boufadel, M.C., 2000. A mechanistic study of nonlinear solute transport in a groundwater-surface water system under steady state and transient hydraulic conditions. Water Resources Research 36, 2549–2565.

Brando, V. E., Braga, F., Zaggia, L., Giardino, C., Bresciani, M., Matta, E., Bellafiore, D., Ferrarin, C., Maicu, F., Benetazzo, A., Bonaldo, D., Falcieri, F. M., Coluccelli, A., Russo, A., Carniel, S., 2015. High-resolution satellite turbidity and sea surface temperature observations of river plume interactions during a significant flood event. Ocean Science 11, 909–920.

British Energy Estuarine & Marine Studies, 2011. Thermal standards for cooling water from new build nuclear power stations. Scientific Advisory Report Series.

Buccino, M., Del Vita, I., Calabrese, M., 2014. Engineering Modeling of Wave Transmission of Reef Balls. Journal of Waterway, Port, Coastal and Ocean Engineering 140 (4), 1-18.

Cardoso-Mohedano, J.G., Bernardello, R., Sanchez-Cabeza, J.A., Ruiz-Fernández, A.C., Alonso-Rodriguez, R., Cruzado, A., 2015. Thermal impact from a thermoelectric power plant on a tropical coastal lagoon. Water, Air, and Soil Pollution 226.

Cavaleri, L., Abdalla, S., Benetazzo, A., Bertotti, L., Bidlot, J.-R., Breivik, Ø., Carniel, S., Jensen, R.E., Portilla-Yandun, J., Rogers, W.E., et al., 2018. Wave modelling in coastal and inner seas. Progress in Oceanography 167, 164–233.

CHC – Canadian Hydraulics Centre, National Research Council, 2010. Blue Kenue. Reference Manual, August 2010.

Chen, C., Shi, P., Mao, Q., 2003. Application of remote sensing techniques for monitoring the thermal pollution of cooling-water discharge from nuclear power plant. Journal of Environmental Science and Health. Part A, Toxic/Hazardous Substances & Environmental Engineering, A38(8), 1659–1668.

Chuang, Y.-L., Yang, H.-H., Lin, H.-J., 2009. Effects of a thermal discharge from a nuclear power plant on phytoplankton and periphyton in subtropical coastal waters. Journal of Sea Research 61, 197-205.

Cooper, P.I., 1969. The absorption of radiation in solar stills. Solar Energy 12, 333–346.

Contini, P., De Girolamo, P., 1998. Impatto Morfologico di Opere a Mare: Casi di Studio (Morphological Impact of Structures at Sea: Case Studies). In: Atti VIII Convegno AIOM, Associazione di Ingegneria Offshore e Marina. Proceedings of 8th Conference of the Offshore and Marine Engineering Association, Lerici, Italy, 85–95.

Cucco, A., Ribotti, A., Olita, A., Fazioli, L., Sorgente, B., Sinerchia, M., Satta, A., Perilli, A., Borghini, M., Schroeder, K., Sorgente, R., 2012. Support to oil spill emergencies in the Bonifacio Strait, western Mediterranean, Ocean Science 8, 443–454.

Delle Rose, M., 2015. Medium-term Erosion Processes of South Adriatic Beaches (Apulia, Italy): A Challenge for an Integrated Coastal Zone Management. J Earth Sci Clim Change 6, 306.

De Dominicis, M., Pinardi, N., Zodiatis, G., Lardner, R., 2013. MEDSLIK-II, a Lagrangian marine surface oil spill model for short-term forecasting – Part 1: Theory, Geosci. Model Dev. 6, 1851–1869.

Dodds, W.K., Whiles, M.R., 2010. Responses to Stress, Toxic Chemicals, and Other Pollutants in Aquatic Ecosystems, Freshwater Ecology (Second Edition). Concepts and Environmental Applications of Limnology Aquatic Ecology, 399–436.

Durán-Colmenares, A., Barrios-Piña, H., Ramírez-León, H., 2016. Numerical Modeling of Water Thermal Plumes Emitted by Thermal Power Plants. Water 8, 482.

Edinger, J.E., Buchak, E.M., 1980. Numerical Hydrodynamics of Estuaries in Estuarine and Wetland Processes with Emphasis on Modeling (P. Hamilton and K. B. Macdonald, eds), 115–146. New York: Plenum.

Egbert, G.D., Erofeeva, S.Y., 2002. Efficient inverse modeling of barotropic ocean tides. J. Atmospheric and Oceanic Technology 19(2), 183–204.

Eldeberky, Y., Battjes, J.A., 1995. Parameterisation of triads interactions in wave energy models. In Proceedings of Coastal Dynamics Conference '95, Gdansk, Poland, 4–8 September 1995, 140–148.

Elwany, M.H.S., Reitzel, J., Erdman, M.R., 1990. Modification of coastal currents by power plant intake and thermal discharge systems. Coastal Engineering 14, 359–383.

Federico, I., Pinardi, N., Coppini, G., Oddo, P., Lecci, R., Mossa, M., 2017. Coastal ocean forecasting with an unstructured grid model in the southern Adriatic and northern Ionian seas, Nat. Hazards Earth Syst. Sci. 17, 45–59.

Franco, L., Archetti, R., 1993. The Italian directional wave measurement network: new insights at the climates off the Mediterranean coasts, Proc. International Conference MED COAST '93, Vol.2, 1197-1211, Ed. E. Ozhan, Antalya, Turkey, November 1993.

Franco, L., 1995. Wave measurements in the Mediterranean Sea, Proc. HYDRA 2000, XXVI IAHR Congress, 3, 162-167, T. Telford, London, Sept. 1995.

Frick, W. E., Roberts, P. J. W., Davis, L. R., Keyes, J., Baumgartner, D. J., George, K. P., 2003.

Dilution Models for Effluent Discharges,4th Edition(Visual Plumes). U.S. Environmental Protection Agency, Office of Research and Development, March.

Gaeta, M.G., Bonaldo, D., Samaras, A.G., Archetti, R., Carniel, S., 2018. Coupled wave - 2D hydrodynamics modeling at the Reno river mouth (Italy) under climate change scenarios. Water 10 (10), 1380.

Gaeta, M.G., Samaras, A.G., Federico, I., Archetti, R., Maicu, F., Lorenzetti, G., 2016. A coupled wave – 3D hydro- dynamics model of the Taranto Sea (Italy): a multiple-nesting approach. Natural Hazards and Earth System Sciences 16 (9), 2071–2083.

Google Earth, 2018. Image © 2018 DigitalGlobe; Data SIO, NOAA, U.S. Navy, NGA, GEBCO; Image © Terrametrics.

Hasselmann, K., Barnett, T.P., Bouws, E., Carlson, H., Cartwright, D.E., Enke, K., Ewing, J.A., Gienapp, H., Hasselmann, D.E., Kruseman, P., et al. 1973. Measurements of wind-wave growth and swell decay during the Joint North Sea Wave Project (JONSWAP). Ergänz. Dtsch. Hydrogr. Z. Reihe 1973, A(8) (Nr. 12), p. 95.

Hervouet, J.M., 2007. Hydrodynamics of free surface flows: modelling with the finite element method, John Wiley & Sons, Ltd, pp. 360.

Ingleton, T., McMinn, A., 2012. Thermal plume effects: A multi-disciplinary approach for assessing effects of thermal pollution on estuaries using benthic diatoms and satellite imagery. Estuarine, Coastal and Shelf Science 99, 132–144.

Israelsson, P.H., Kim, Y.D., Adams, E.E., 2006. A comparison of three Lagrangian approaches for extending near field mixing calculations. Environmental Modelling & Software 21, 1631–1649.

James, I.D., 2002. Modelling pollution dispersion, the ecosystem and water quality in coastal waters: a review. Environmental Modelling & Software 17, 363–385.

Jirka, G.H., Doneker, R.L., Hinton, S.W., 1996. User's manual for CORMIX: A hydrodynamic mixing zone model and decision support system for pollutant discharges into surface waters, Tech. Rep., Environment.

Jordi, A., Wang, D.P., 2012. sbPOM: a parallel implementation of Princenton Ocean Model. Environmental Modelling & Software 38, 59–61.

Kim, B.K., Jeong, Y.H., 2013. High cooling water temperature effects on design and operational safety on NPPS in the Gulf Region, Nuclear Engineering and Technology 45 (7), 961–968.

Kolluru, V., Buchak, E., Brinkmann, P., 2003. Hydrodynamic Modeling of Coastal LNG Cooling Water Discharge. Journal of Energy Engineering 129, 16–31.

Lardicci, C., Rossi, F., Maltagliati, F., 1999. Detection of thermal pollution: Variability of benthic communities at two different spatial scales in an area influenced by a coastal power station. Marine Pollution Bulletin 38, 296–303.

Li, X.Y., Li, B., Sun, X.L., 2014. Effects of a coastal power plant thermal discharge on phytoplankton community structure in Zhanjiang Bay, China. Marine Pollution Bulletin 81, 210–217.

Longuet-Higgins, M.S., Steward, R.W., 1964. Radiation stresses in water waves; a physical discussion with applications. Deep-Sea Res. 11, 529–562.

Luck, M., Guesmia, M., 2002. SUBIEF-3D Version 5.3, Manuel de l'utilisateur, HP-75/02/086/A. EDF R& D LNHE.

Maderich, V., Heling, R., Bezhenar, R., Brovchenko, I., Jenner, H., Koshebutskyy, V., Kuschan, A., Terletska, K., 2008. Development and application of 3D numerical model THREETOX to the prediction of cooling water transport and mixing in the inland and coastal waters. Hydrological Processes 22, 1000–1013.

Manivanan, R., Singh, C.B., 2013. Modelling of diffusion and dispersion of hot water discharge vis-à-vis hydrothermal-informatics. Pluraridade 2013, 2, 57–67.

Matta, E, Selge, F., Gunkel, G., Hinkelmann, R., 2017. Three-Dimensional Modeling of Wind- and Temperature-Induced Flows in the Icó-Mandantes Bay, Itaparica Reservoir, NE Brazil. Water 9, 772.

MATTM, Italian Minister of Environment. http://www.pcn.minambiente.it/mattm/progetto-coste/, last access 20/10/2018.

Muthulakshmi, A.L., Natesan, U., Ferrer, V.A., Deepthi, K., Venugopalan, V.P., Narasimhan, S.V., 2013. A novel technique to monitor thermal discharges using thermal infrared imaging. Environmental Sciences: Processes and Impacts 15, 1729–1734.

Panin, G.N., Brezgunov, V.S., 2007. Influence of the salinity of water on its evaporation. Izvestiya, Atmospheric and Oceanic Physics 43, 663–665.

Poornima, E.H., Rajadurai, M., Rao, T.S., Anupkumar, B., Rajamohan, R., Narasimhan, S.V., Rao, V.N.R., Venugopalan, V.P., 2005. Impact of thermal discharge from a tropical coastal power plant on phytoplankton. Journal of Thermal Biology 30, 307–316.

Rosati, A., Miyakoda, K., 1988. A General Circulation Model for Upper Ocean Simulation. Journal of Physical Oceanography, 18, 1601–1626.

Rosen, M.A., Bulucea, C.A., Mastorakis, N.E., Bulucea, C.A., Jeles, A.C., Brindusa, C.C., 2015. Evaluating the Thermal Pollution Caused by Wastewaters Discharged from a Chain of Coal-Fired Power Plants along a River. Sustainability 7, 5920–5943.

Samaras, A.G., De Dominicis, M., Archetti, R., Lamberti, A., Pinardi, N., 2014. Towards improving the representation of beaching in oil spill models: A case study. Marine Pollution Bulletin 88, 91–101.

Samaras, A.G., Gaeta, M.G., Miquel, A.M., Archetti, R., 2016. High-resolution wave and hydrodynamics modelling in coastal areas: operational applications for coastal planning, decision support and assessment. Nat. Hazards Earth Syst. Sci. 16, 1499–1518.

Schreiner, S.P., Krebs, T.A., Strebel, D.E., Brindley, A., 2002. Testing the CORMIX model using thermal plume data from four Maryland power plants. Environmental Modelling & Software 17, 321–331.

Simmons, J.A., Marshall, L.A., Turner, I.L., Splinter, K.D., Cox, R.J., Harley, M.D., Hanslow, D.J., Kinsela, M.A., 2015. A more rigorous approach to calibrating and assessing the uncertainty of coastal numerical mod- els. Australasian Coasts & Ports Conference 2015: 22nd Australasian Coastal and Ocean Engineering Conference and the 15th Australasian Port and Harbour Conference. Auckland, New Zealand: Engineers Australia and IPENZ: 821–827.

Schaltout, M., Omstedt, A., 2014. Recent sea surface temperature trends and future scenarios for the Mediterranean Sea. Oceanologia 56(3), 411–443.

Stamou, A.I., Nikiforakis, I.K., 2013. Integrated modelling of single port, steady-state thermal discharges in unstratified coastal waters. Environmental Fluid Mechanics 13, 309–336.

Suh, S.W., 2006. A hybrid approach to particle tracking and Eulerian–Lagrangian models in the simulation of coastal dispersion. Environmental Modelling & Software 21, 234–242.

Suh, S.W., 2014. Massive cooling water dispersion behavior in a shallow macro-tidal coastal zone in Korea. J. Coastal Res. 70, 360–365.

Suh, S.W., 2001. A hybrid near-field/far-field thermal discharge model for coastal areas. Marine Pollution Bulletin 43, 225–233.

Tang, H.S., Paik, J., Sotiropoulos, F., Khangaonkar, T., 2008. Three-dimensional numerical modeling of initial mixing of thermal discharges at real-life configurations. Journal of Hydraulic Engineering 134, 1210–1224.

TELEMAC. The Mathematically Superior Suite of Solvers, 2017. Available online: http://www.opentelemac.com (last access on 10 April 2019).

Trotta, F., Fenu, E., Pinardi, N., Bruciaferri, D., Giacomelli, L., Federico, I., Coppini, G., 2016. A Structured and Unstructured grid Relocatable ocean platform for Forecasting (SURF), Deep-Sea Research Part II: Topical Studies in Oceanography 133, 54–75.

Wu, J., Buchak, E.M., Edinger, J.E., Kolluru, V.S., 2001. Simulation of cooling-water discharges from power plants. Journal of Environmental Management 61, 77–92.